

Leaky Partial Updates to Control a Real Device Casing

Dariusz BISMOR 

Department of Measurements and Control Systems, Silesian University of Technology, ul. Akademicka 16,
44-100 Gliwice, Poland

Corresponding author: Dariusz BISMOR, email: Dariusz.Bismor@polsl.pl

Abstract Structural active noise control (ANC) is one of few solutions applicable when global noise reduction is required: control of a whole device casing allows to lower the acoustic energy emitted by this device. Unfortunately, structural ANC usually requires a large number of sensors and actuators, making the control system multichannel with large dimensionality. This in turn presents a huge computational power demands. There are several ways to lower this demand, the partial updates being one of them. The goal of this paper is to show applicability of the leaky partial update LMS algorithms in structural ANC of a washing machine casing. The transfer functions of the numerous device paths were identified using a real washing machine in the ANC laboratory. The identified transfer functions allowed to create a simulation system, where different algorithms could be easily tested. The results of the simulations confirm effectiveness of the proposed solution.

Keywords: structural active noise control, partial updates, leaky LMS, signal processing.

1. Introduction

Many home appliances produce unwanted noise during their operation. The annoyance of such noise depends on both its level and frequency of its occurrence. Dishwashers and washing machines are engaged very frequently, even if they do not produce very high levels of sound. The exception is the spin drying phase with high rotation speed, which can produce sound levels up to 70 dB. Considering the above, a reduction of noise generated by washing machines and dishwashers is an important task, directly affecting the quality of life of household members [6, 7]. Due to spectral content of such noise, this task involves active noise control (ANC) methods.

As well known, ANC allows to control noise at lower frequency ranges, compared to passive methods. However, a frequent drawback of spatial ANC systems is that the attenuation of noise in one area of the space is associated with the amplification of noise in another area. This drawback does not apply to structural methods, which allow to obtain a global noise control effect [11, 9, 8]. Unfortunately, a structural ANC system usually needs to be multichannel, with many actuators placed on the structure under control. Many publications indicate that at least 3 error sensors and 3 actuators must be used for effective control [9, 10]. Other publications show that it is impossible to disregard the coupling between control paths concerned with different walls (i.e. apply 3 independent, single-channel systems), as it usually results in an unstable operation. The above issues suggest that the computational demands of structural ANC system are high, challenging even for modern, multiprocessor hardware [4].

There are several ways of lowering the computational demand, e.g. using shorter filters, using switched error, etc. However, partial parameter updates is a new technique that recently gathers more attention [2, 3]. The technique, which can be applied to any iterative algorithm, depends on updating only a selected subset of an adaptive filter parameters. Partial updates (PU) is usually applied to any version of the LMS algorithm (e.g., LMS, NLMS, FxLMS). This paper shows how PU can be used in a structural ANC system, where the structure under control is a washing machine.

2. Leaky LMS Partial Updates

Partial updates were developed to be used with algorithms without leakage [5]. Recently, however, leaky versions of PU LMS algorithms were presented and proved to work [4]. The details of these algorithm are presented in the above paper, but for convenience of the reader the main facts on leaky PU algorithms are summarized below.

The equation describing leaky LMS PU can be given as:

$$\mathbf{w}(n+1) = \mathbf{G}_M(n)\mathbf{w}(n) - \mu\mathbf{I}_M(n)\mathbf{u}(n)e(n), \quad (1)$$

where $\mathbf{w}(n+1)$ is the vector of filter coefficients of size L in iteration n , $\mathbf{G}_M(n)$ is the leakage matrix, μ is the step size, $\mathbf{I}_M(n)$ is the coefficient selection matrix, $\mathbf{u}(n)$ is the vector of input signal samples and $e(n)$ is the error.

The coefficient selection matrix $\mathbf{I}_M(n)$ is a diagonal matrix with elements on the diagonal equal to 1, if a corresponding coefficient is selected for update, or 0, if not. The number of coefficients to be updated in each iteration is equal to $M < L$. A particular parameter is selected for the update in a given iteration based on the selected PU algorithm. The leakage matrix $\mathbf{G}_M(n)$ is a diagonal matrix as well and it contains elements equal to 1 in the rows corresponding to 0-s in the $\mathbf{I}_M(n)$ matrix, and a selected value of the leakage γ in the rows corresponding to 1-s in the coefficient selection matrix.

The PU algorithms can be roughly divided into data-independent and data-dependent algorithms. The first group contains the algorithms offering the highest computational savings, which are obtained at the cost of the convergence speed. A representative of the algorithms from this group selected for this study is the sequential LMS algorithm. The second group includes the algorithms that select parameters for update based on the input data. As this requires some insight into the input data, which in turn is associated with some computations, these algorithms offer less computational savings, compared to the previous group. However, the algorithms do not suffer so much from the convergence speed drop. This study includes three algorithms from this group, which proved to be the most effective during previous research: M-max LMS, M-max NLMS and the Selective NLMS algorithms.

3. Experimental setup

The setup being the base for the experiments described below consisted of a commercial washing machine, which was positioned as close as possible to one of the laboratory room walls—see Fig. 1a. Therefore, only four washing machine walls were controlled: front, left, right and top. Each wall was equipped with 5 W electrodynamic actuators: there were three actuators on the side walls and four on the top. A reference microphone was placed inside the washing machine, below the drum, and eight error microphones were located in the laboratory, in a quarter-sphere arrangement [6]. The setup allowed to identify 256 parameters-long impulse responses of primary and secondary paths: there were eight primary paths (from the reference microphone to each of the eight error microphones) and 104 secondary paths (from each of the thirteen actuators to each of the eight error microphones). The sampling frequency of 2 kHz was used. The primary path transfer functions (TF) will be named $P_y(z^{-1})$, where y is the error microphone number, and the secondary path TF will be named $S_{x,y}(z^{-1})$, where x is the actuator number ($x \in \{1..13\}$), and y is again the error microphone number. Secondary path TF frequency responses between the front wall actuators and the first error microphone are presented in Fig. 2a, while those between the top wall actuators and the third error microphone are presented in Fig. 2b.

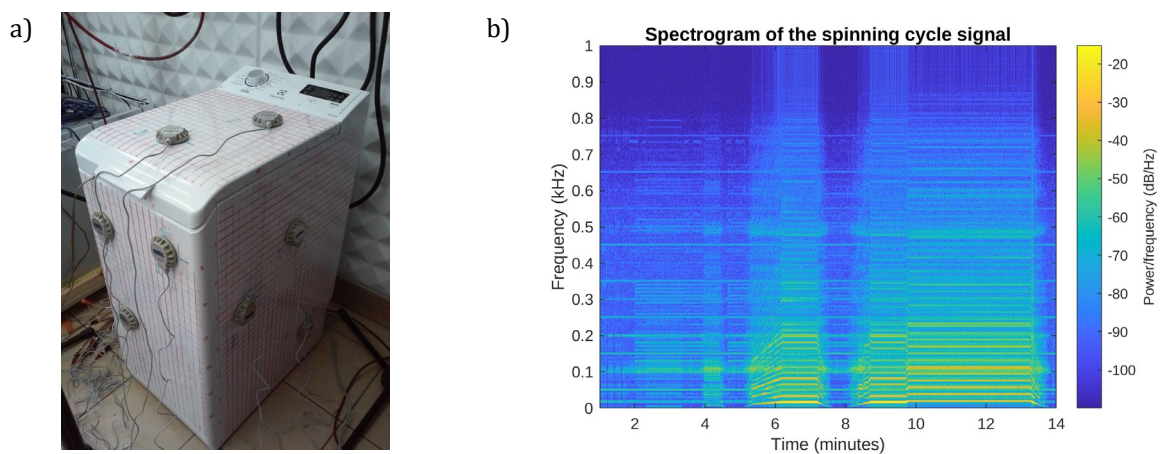


Figure 1. a) The washing machine used in the experiments.
b) Spectrogram of the signal recorded during the washing machine final spinning phase.

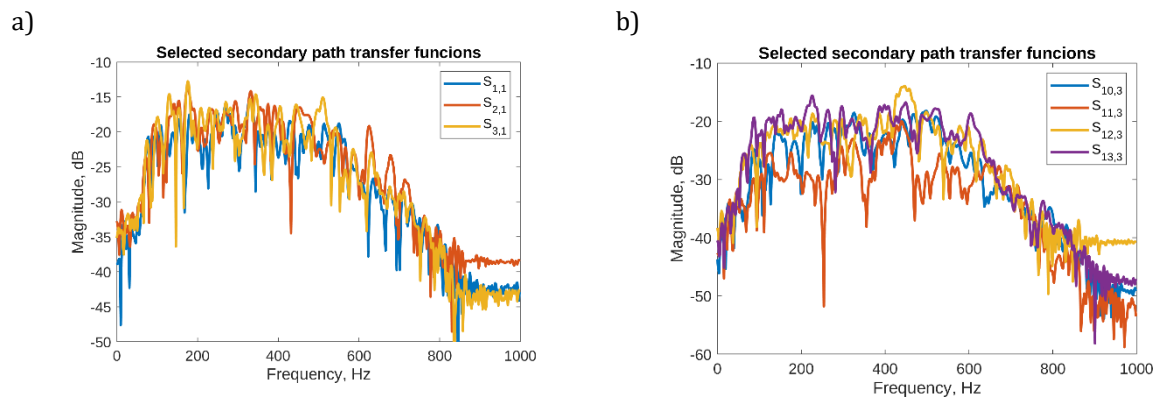


Figure 2. Secondary path transfer functions: a) from the front plate actuators to the front plate error microphone, b) from the top plate actuators to the front plate error microphone.

Figure 3 presents the part of the block diagram of the control system, associated with one plate (front) and one error signal. The primary signal, $u(n)$, is filtered through the reference path transfer function, $X(z^{-1})$, to produce the reference signal, $x(n)$. This reference signal forms the input signal to the three control filters attached to the front plate. Each control filter produces the output which is then filtered with eight different secondary path transfer functions; one of these functions for each filter is visible on the figure (i.e. $S_{1,1}(z^{-1})$, $S_{2,1}(z^{-1})$, and $S_{3,1}(z^{-1})$), while the remaining seven belong to the other error signal paths. Thus, each error signal is a sum of 14 signals: one primary and 13 signals coming from the 13 actuators. All the 8 error signals are used by each of the adaptation algorithms (denoted as LMS), together with the 8 reference signals, each filtered through a different secondary path transfer function estimate.

For the experiments presented below, the system was parametrized as follows. The length of the control filters used was 256. The step size used with the non-normalized adaptation algorithms was equal to 0.01, while the normalized step size was equal to $2 \cdot 10^{-8}$. The step sizes were experimentally adjusted with a great care to achieve as fast as possible convergence speed, but to avoid unwanted effects that frequently appear in ANC systems with too large step sizes [1]. The leakage factor was set to 0.999999—a value which worked well in all simulations. Finally, ideal secondary path transfer function estimates were used to avoid an additional factor with uncertain influence.

4. Simulation results

The simulations were performed using a signal recorded during the washing machine final spinning cycle, which is the loudest washing process phase [8]. The spectrogram of the signal recorded during this phase at the reference microphone is shown in Fig. 1b. The spinning signal spectrum main component is 114 Hz and is connected to the 6th harmonic of the drum spinning frequency. For clarity of the presentation, only the last 5 minutes of the signal are presented in the simulation results.

Figure 4a presents the errors obtained with the Leaky Normalized LMS algorithm, which are presented as a reference. To make this paper compact, only four (out of eight) errors are presented, together with the primary noise, i.e. the reference signal filtered through a corresponding primary path. Observe different levels of signals on each microphone, which are the result of different amplification of each primary path. However, in case of each microphone the attenuated signal envelope is smaller than the primary noise. The actual attenuation levels, calculated for the last quarter of the signal, are summarized in Table 1.

Figures 4b–6 present the results obtained for the PU algorithm considered in this paper, with $M = 16$, i.e. sixteen filter parameters were updated in each simulation step (out of 256). The exception is the One Tap Update algorithm, which updates only one filter tap in each step. From the figures it can be concluded that the algorithms performed as expected: the data-independent algorithm (Sequential LLMS) resulted in significantly slower convergence, while the data-dependent algorithms performance was comparable with the Leaky NLMS algorithm. A special attention should be paid to the OTU LLMS algorithm, which also resulted in similar performance, while updating only one tap in each iteration.

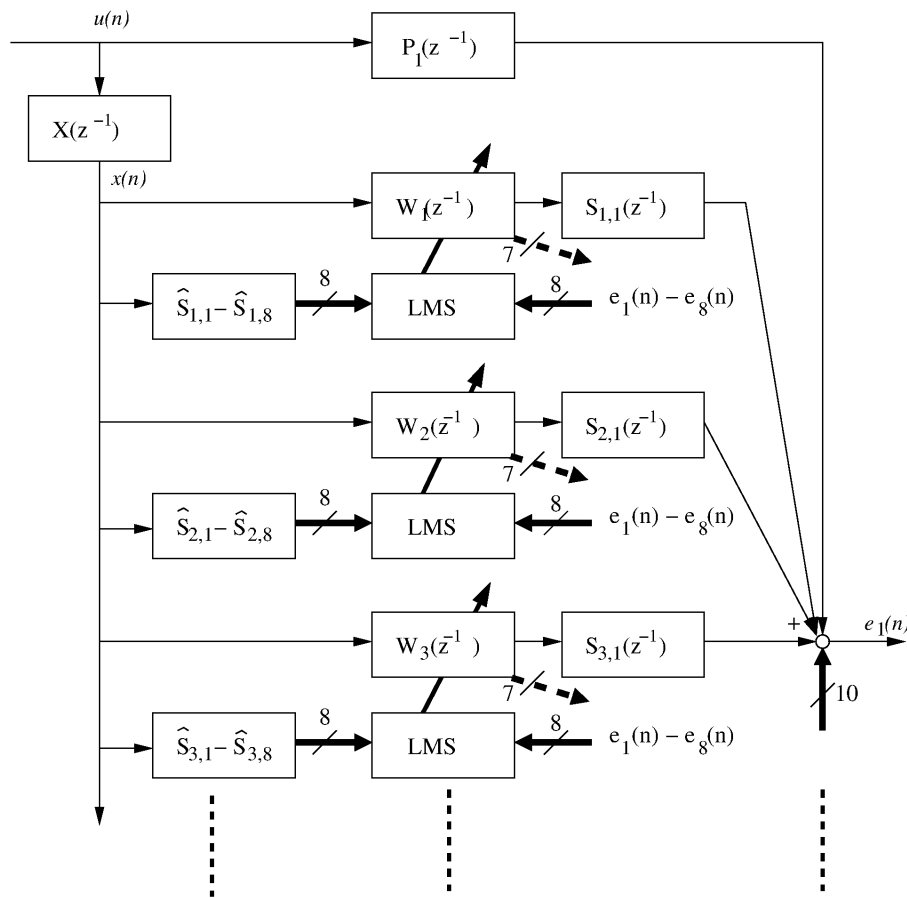


Figure 3. The block diagram of the ANC system.

Comparison of the performance of the PU algorithms for a selected error signal (e_5) is presented in Fig. 7a (algorithms without the step size normalization) and in Fig. 7b (algorithms with the step size normalization). From the figures it comes that the Selective LNLMS algorithm and the OTU LNLMS algorithm appear to be slightly divergent towards the end of the simulation. This may be easily avoided by decreasing the step size, but observe also that the simulation ends with the end of the spinning cycle, and the next condition may make the adaptive filter convergent again.

Figures 14 and 15 present the spectra of the portion of the signal towards the end of the simulation without and with the attenuation. The spectra are presented for the error microphone with the worst (e_4) and the best (e_5) attenuation factor. Observe that the main harmonics are significantly reduced, by 20–30 dB. Observe also that the signal level is lower in case of e_4 , what justifies worse attenuation: the final signal levels are comparable in spite of this difference.

Table 1. Attenuation levels obtained for each error microphone for $M = 16$.

| Algorithm | e_1 | e_2 | e_3 | e_4 | e_5 | e_6 | e_7 | e_8 |
|-----------------|---------|---------|---------|---------|---------|---------|---------|---------|
| LLMS | 9.5 dB | 11.0 dB | 12.5 dB | 7.7 dB | 19.4 dB | 13.0 dB | 14.9 dB | 8.4 dB |
| LNLMS | 10.3 dB | 15.5 dB | 13.4 dB | 10.5 dB | 23.5 dB | 16.3 dB | 17.6 dB | 17.4 dB |
| Sequential LLMS | 4.8 dB | 5.7 dB | 7.2 dB | 3.3 dB | 11.0 dB | 6.6 dB | 7.0 dB | 3.5 dB |
| mMax LLMS | 7.5 dB | 8.9 dB | 9.9 dB | 5.8 dB | 15.9 dB | 10.4 dB | 11.6 dB | 5.8 dB |
| mMax LNLMS | 7.2 dB | 11.8 dB | 11.7 dB | 5.7 dB | 17.4 dB | 12.2 dB | 13.1 dB | 12.4 dB |
| Selective LLMS | 9.5 dB | 12.5 dB | 13.4 dB | 7.7 dB | 23.0 dB | 13.4 dB | 16.1 dB | 16.1 dB |
| OTU LNLMS | 9.2 dB | 12.6 dB | 12.0 dB | 8.9 dB | 19.0 dB | 13.4 dB | 13.8 dB | 14.0 dB |

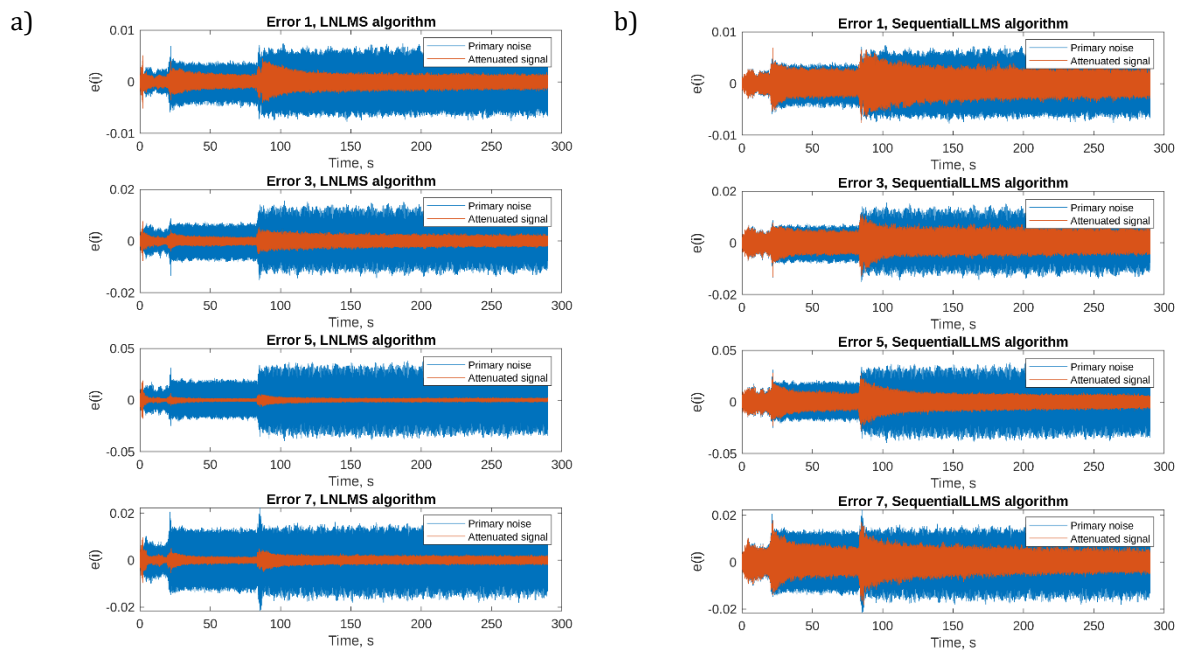


Figure 4. Simulation results: a) the Leaky NLMS algorithm, b) the Sequential Leaky LMS algorithm, $M=16$.

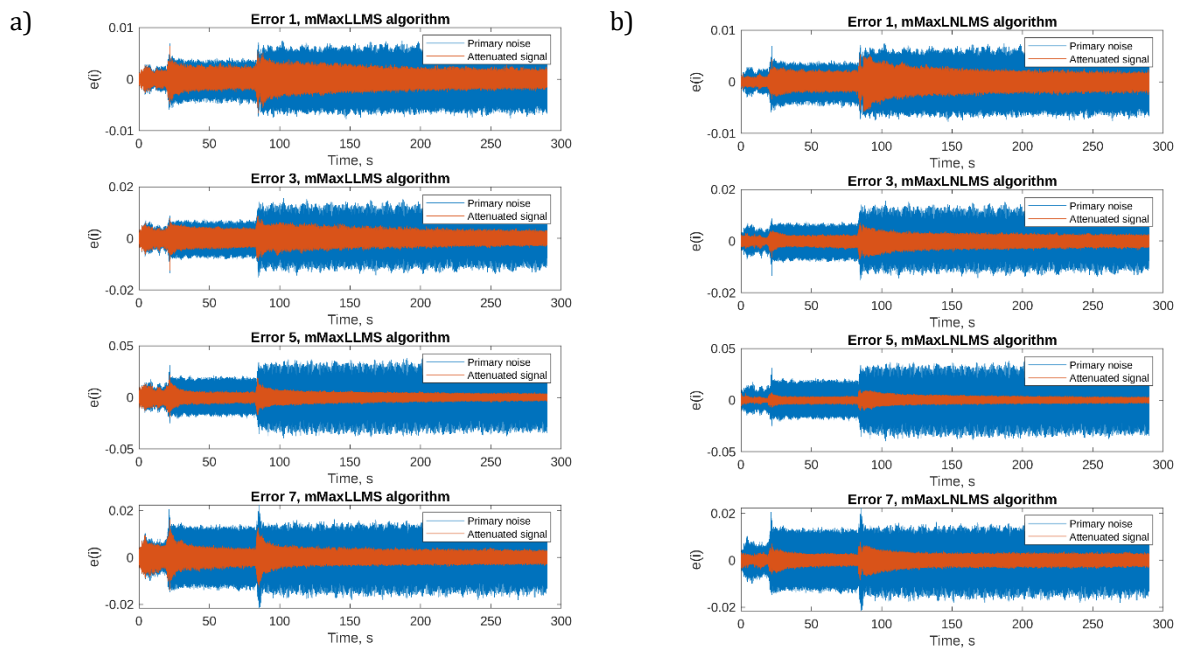


Figure 5. Simulation results: a) the mMax Leaky LMS algorithm, $M=16$
b) the mMax Leaky LNLS algorithm, $M=16$.

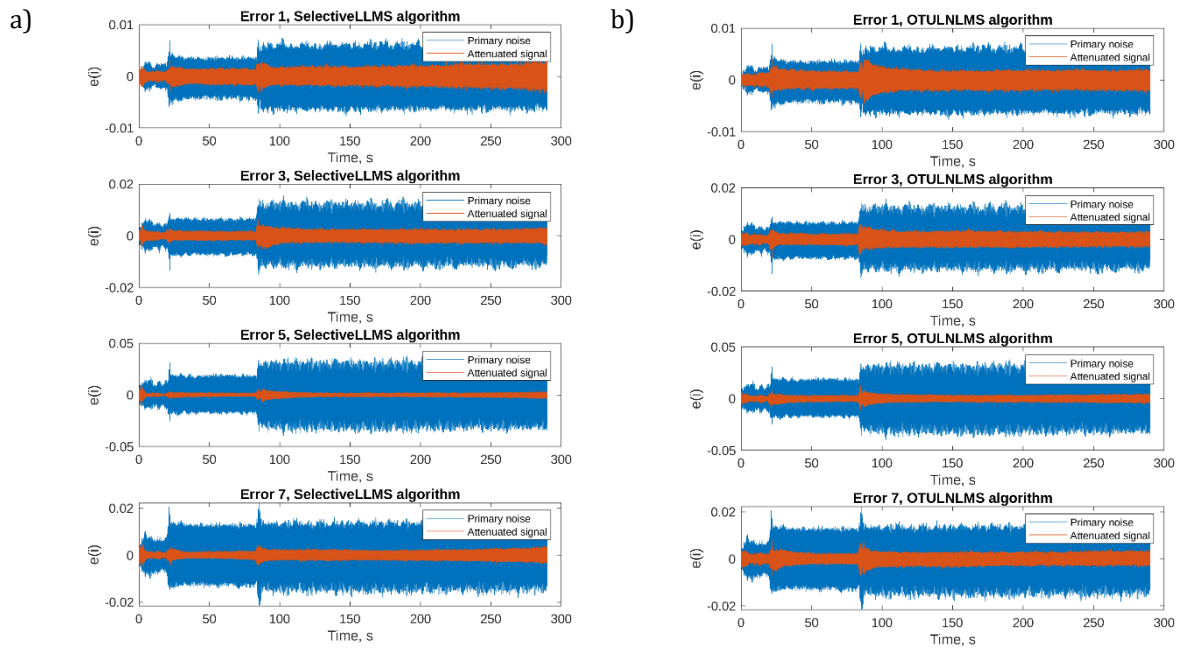


Figure 6. Simulation results: a) the Selective Leaky NLMS algorithm, $M=16$
 b) the One Tap Update algorithm.

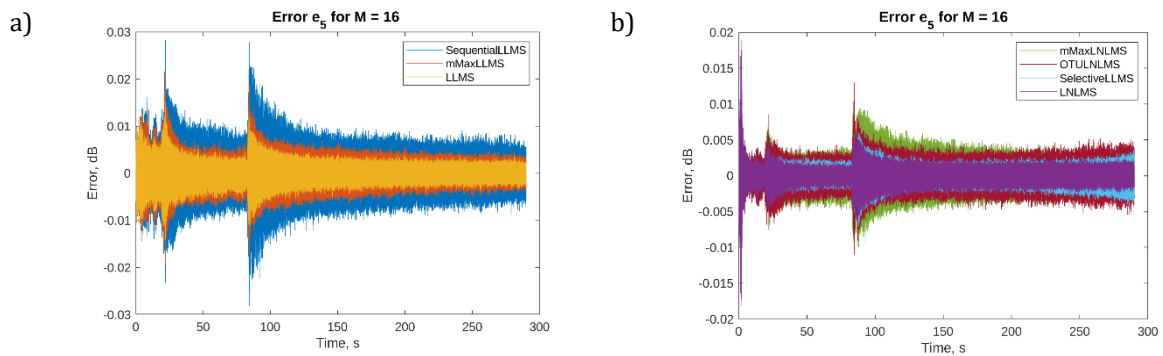


Figure 7. Comparison of simulation results for algorithms: a) without,
 b) with the step size normalization, $M=16$.

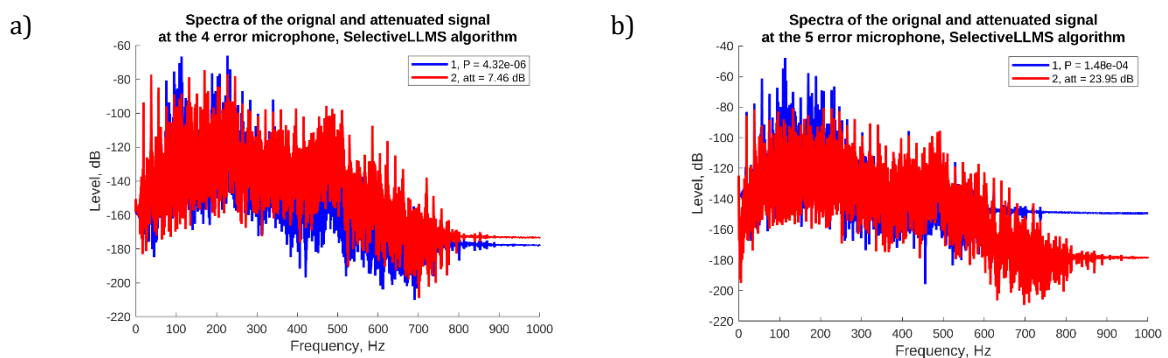


Figure 8. Spectrum of the error signal before and after the attenuation: a) $e_4(i)$, b) $e_5(i)$.

Table 2. Attenuation levels obtained for each error microphone for $M = 8$.

| Algorithm | e ₁ | e ₂ | e ₃ | e ₄ | e ₅ | e ₆ | e ₇ | e ₈ |
|-----------------|----------------|----------------|----------------|----------------|----------------|----------------|----------------|----------------|
| Sequential LLMS | 3.9 dB | 4.9 dB | 6.4 dB | 2.5 dB | 9.2 dB | 5.6 dB | 5.5 dB | 2.7 dB |
| mMax LLMS | 6.5 dB | 7.8 dB | 8.8 dB | 4.9 dB | 14.5 dB | 9.2 dB | 10.2 dB | 5.1 dB |
| mMax LNLMS | 5.6 dB | 11.1 dB | 9.6 dB | 4.5 dB | 15.8 dB | 11.1 dB | 11.8 dB | 10.6 dB |
| Selective LLMS | 8.8 dB | 12.1 dB | 11.9 dB | 7.6 dB | 21.1 dB | 13.1 dB | 14.4 dB | 14.8 dB |

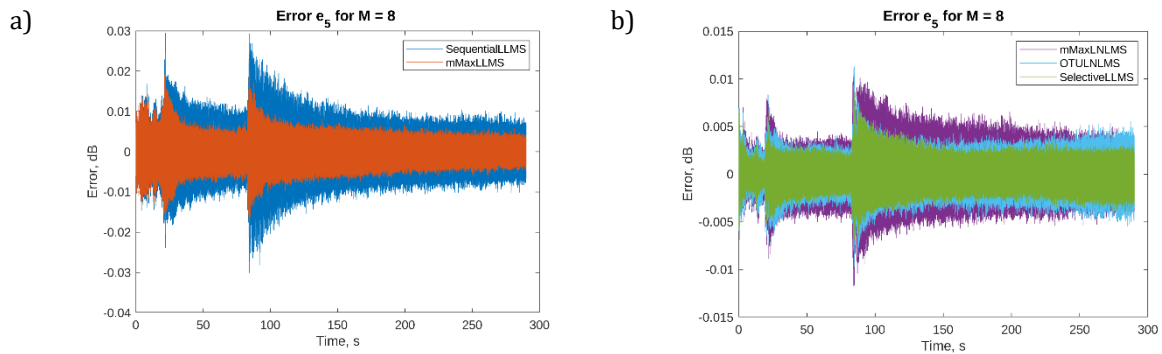


Figure 9. Comparison of simulation results for algorithms:
a) without, b) with the step size normalization, $M=8$.

Table 2 summarizes the attenuation obtained for $M = 8$ (eight taps updated in each iteration), for the algorithms depending on this selection. Comparing the results with the reference algorithms (with full update, see Table 1) can be concluded that the final attenuation is now significantly worse for all algorithms but the Selective LNLMS algorithm. However, the results obtained with both the mMax algorithms are also not bad and can be accepted as a compromise between the performance and computational demands. Figures 9a and 9b show the plots of the signals obtained during the simulation at microphone 5.

Table 3. Attenuation levels obtained for each error microphone for $M = 4$.

| Algorithm | e ₁ | e ₂ | e ₃ | e ₄ | e ₅ | e ₆ | e ₇ | e ₈ |
|-----------------|----------------|----------------|----------------|----------------|----------------|----------------|----------------|----------------|
| Sequential LLMS | 2.9 dB | 4.2 dB | 5.4 dB | 1.7 dB | 7.1 dB | 4.7 dB | 4.0 dB | 2.0 dB |
| mMax LLMS | 5.5 dB | 6.6 dB | 7.7 dB | 3.9 dB | 12.8 dB | 7.9 dB | 8.7 dB | 4.2 dB |
| mMax LNLMS | 4.8 dB | 10.6 dB | 8.1 dB | 4.3 dB | 14.6 dB | 10.2 dB | 10.4 dB | 9.8 dB |
| Selective LLMS | 7.8 dB | 11.5 dB | 11.6 dB | 7.4 dB | 20.6 dB | 13.1 dB | 13.6 dB | 13.9 dB |

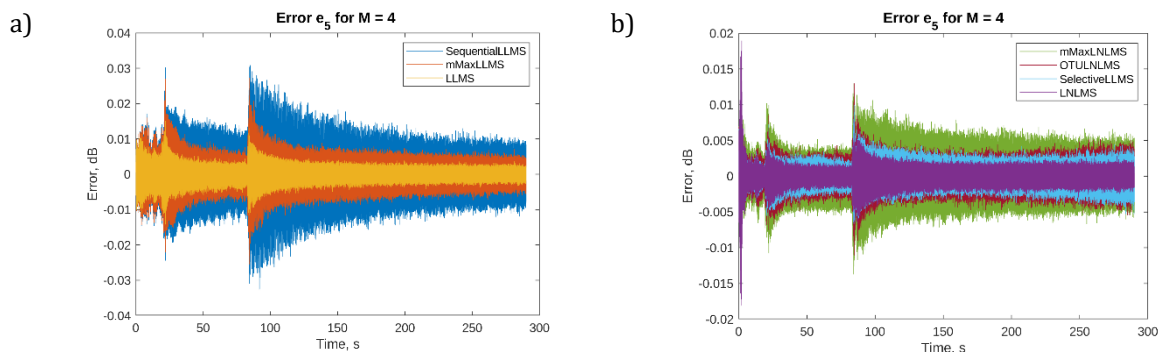


Figure 10 Comparison of simulation results for algorithms:
a) without, b) with the step size normalization, $M=4$.

Finally, the results obtained with $M = 4$ are presented in Table 3 and in Figs. 10a–10b. In this case only the performance of the Selective LNLMS algorithm seems to be acceptable for this application.

4. Conclusions

The simulations being the basis for this short article prove that the Partial Update LMS algorithms can be successfully applied to the structural ANC application, where a commercial washing machine or similar appliance is under control. The algorithms can be used with the leakage, which is usually crucial for a multichannel ANC system, and allows to avoid filter output overflow. In case of data-independent algorithms, which offer the best computational power savings, updating one of each 16 filter parameters (i.e. updating 16 parameters in each iteration for 256-tap filter) results in good performance measured as convergence speed and final attenuation. The data-dependent algorithms (e.g. mMax or Selective algorithms) can be used even with $M = 8$ or 4. A particularly interesting algorithm is the One Tap Update algorithm, which is a special case of the Selective algorithm, with $M = 1$. It allows to update only one (but carefully selected) parameter, but still maintain a good performance.

Acknowledgments

The research reported in this paper has been supported by the National Science Centre, Poland, decision No. DEC2017/25/B/ST7/02236.

Additional information

The author(s) declare: no competing financial interests and that all material taken from other sources (including their own published works) is clearly cited and that appropriate permits are obtained.

References

1. D. Bismor; Comments on "A new feedforward hybrid ANC system"; IEEE Signal Processing Letters 2014, 21(5), 635–637. DOI: 10.1109/LSP.2014.2310783
2. D. Bismor; Partial update LMS algorithms in active noise control; In Proceedings of Forum Acusticum 2014, Kraków, pages 1–7.
3. D. Bismor; Simulations of partial update LMS algorithms in application to active noise control. Procedia Computer Science 2016, 80, 1180–1190. International Conference on Computational Science 2016, ICCS 2016, 6-8 June 2016, San Diego, California, USA. DOI: 10.1016/j.procs.2016.05.451
4. D. Bismor; Leaky Partial Updates in Application to Structural Active Noise Control, in Postępy akustyki, E. Czajka, I. Suder-Dębska Eds.; Polskie Towarzystwo Akustyczne, Oddział w Krakowie, Kraków, 2021, 44–53.
5. K. Doğançay; Partial-Update Adaptive Signal Processing. Design, Analysis and Implementation. Academic Press: Oxford, 2008.
6. K. Mazur, M. Pawelczyk; Active control of noise emitted from a device casing; Proceedings of the 22nd International Congress on Sound and Vibration, Florence, Italy, 2015.
7. K. Mazur, S. Wrona, M. Pawelczyk; Active noise control for a washing machine; Applied Acoustics 2019, 146, 89 – 95. DOI: 10.1016/j.apacoust.2018.11.010
8. K. Mazur, S. Wrona, M. Pawelczyk; Performance evaluation of active noise control for a real device casing; Applied Sciences 2020, 10(1). DOI: 10.3390/app10010377
9. S. Wrona, M. de Diego, and M. Pawelczyk; Shaping zones of quiet in a large enclosure generated by an active noise control system; Control Engineering Practice 2018, 80, 1–16. DOI: 10.1016/j.conengprac.2018.08.004
10. S. Wrona and M. Pawelczyk; Shaping frequency response of a vibrating plate for passive and active control applications by simultaneous optimization of arrangement of additional masses and ribs. Part ii: Optimization; Mechanical Systems and Signal Processing 2016, 70-71, 699–713. DOI: 10.1016/j.ymsp.2015.08.017
11. J. Wyrwal, M. Pawelczyk, L. Liu, Z. Rao; Double-panel active noise reducing casing with noise source enclosed inside — modelling and simulation study; Mechanical Systems and Signal Processing 2021, 152, 107371. DOI: 10.1016/j.ymsp.2020.107371

© 2022 by the Authors. Licensee Poznan University of Technology (Poznan, Poland). This article is an open access article distributed under the terms and conditions of the Creative Commons Attribution (CC BY) license (<http://creativecommons.org/licenses/by/4.0/>).